

Supplementary Materials for
Structure of *Saccharomyces cerevisiae* Rtr1 reveals an active site for an atypical phosphatase

Seema Irani, S. D. Yogेशa, Joshua Mayfield, Mengmeng Zhang, Yong Zhang,
Wendy L. Matthews, Grace Nie, Nicholas A. Prescott, Yan Jessie Zhang*

*Corresponding author. E-mail: jzhang@cm.utexas.edu

Published 1 March 2016, *Sci. Signal.* **9**, ra24 (2016)
DOI: 10.1126/scisignal.aad4805

The PDF file includes:

- Fig. S1. Activity toward *p*NPP requires prolonged incubation with *S. cerevisiae* Rtr1.
- Fig. S2. Electrospray ionization mass spectrometry analysis of Rtr1₁₋₂₁₃ in a buffer containing phosphate.
- Fig. S3. The purification of Rtr1₁₋₁₇₈ using size exclusion chromatography.
- Fig. S4. Gel filtration profile and SDS-PAGE of Rtr1₁₋₂₁₃ mutation variants with low in vitro activity.
- Fig. S5. The presence of zinc in Rtr1₁₋₁₇₈ crystals.
- Fig. S6. Surface representation of *S. cerevisiae* Rtr1₁₋₁₇₈.
- Fig. S7. The electron density of sulfate molecule at site 1 in the Rtr1₁₋₁₇₈ structure.
- Fig. S8. Comparison of protein folding in different phosphatases families.
- Fig. S9. Comparison of the active site of Scp1 and Rtr1.
- Table S1. Analysis of stability and activity of Rtr1 and the mutants.
- Table S2. Analysis of stability and activity of RPAP2.

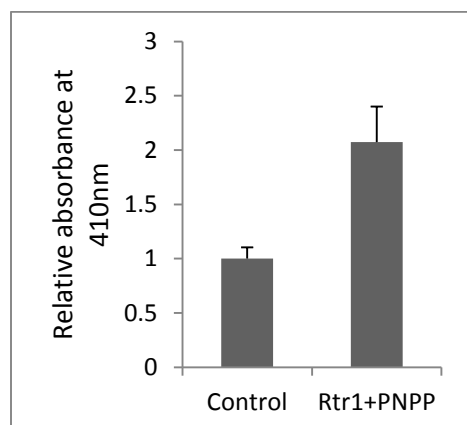


Figure S1: Activity toward *p*NPP requires prolonged incubation with *S. cerevisiae* Rtr1. Truncated Rtr1₁₋₂₁₃ at 28 μ M concentration was incubated with 50 mM *p*NPP for 16 hours. The OD was measured at 410 nm. The values indicate the average of three independent experiments performed in duplicate and the standard deviation is shown as error bars.

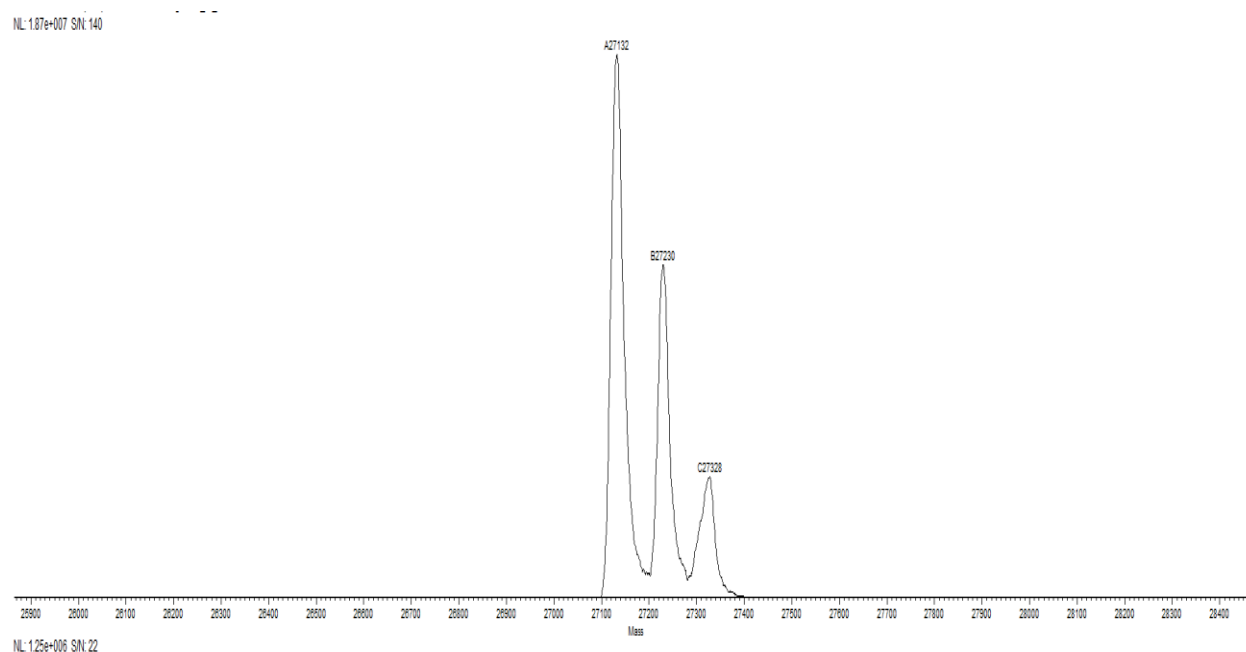
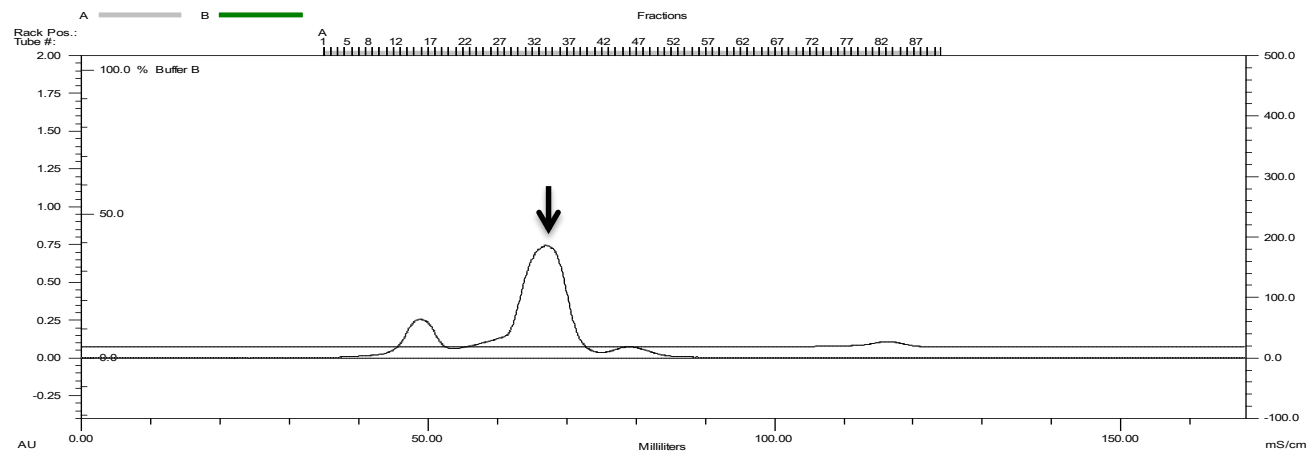
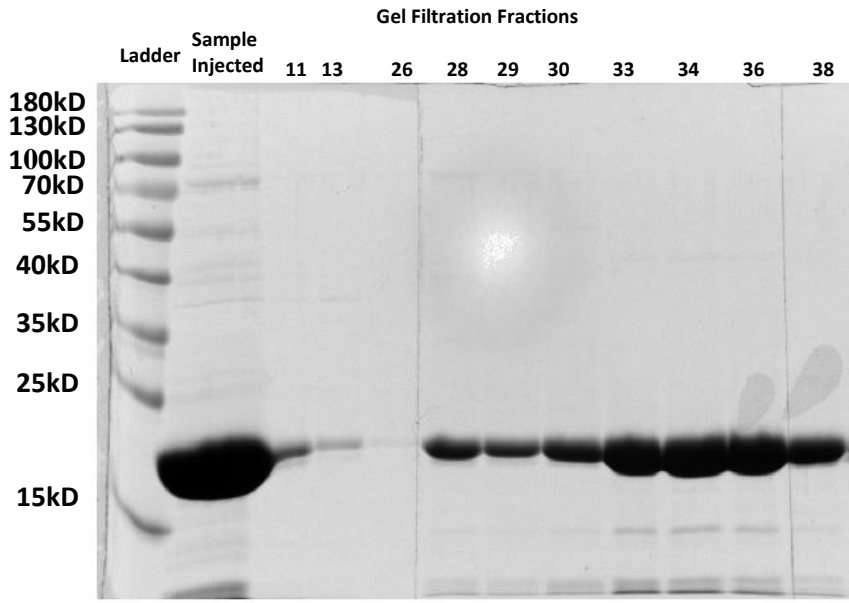


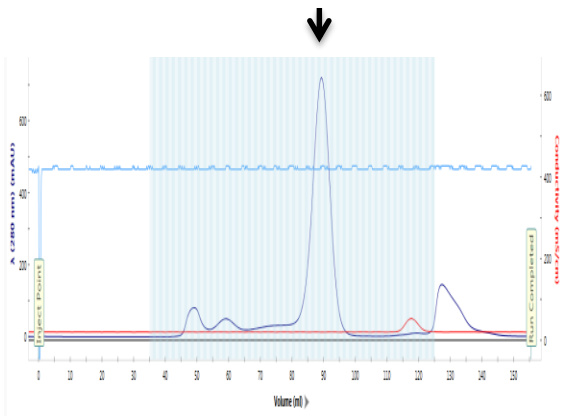
Figure S2: Electrospray ionization mass spectrometry analysis of Rtr1₁₋₂₁₃ in a buffer containing phosphate. Shown are the zoomed-in images of the deconvoluted peak of the proteins, which shows as a triplet peak. The left peak of 27,132 Da corresponding to Rtr1₁₋₂₁₃ (theoretical MW of 27,129 Da). The middle peak is 96 Da heavier than Rtr1₁₋₂₁₃, which is consistent with the noncovalent association of a molecule of inorganic phosphate. The right peak is another 96 Da heavier than the middle peak, implying a second phosphate associated with Rtr1₁₋₂₁₃.



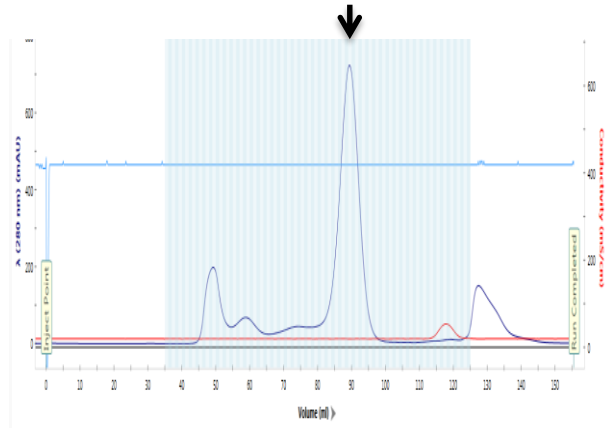
Rtr1₁₋₁₇₈ gel filtration Profile

Figure S3: The purification of Rtr1₁₋₁₇₈ using size exclusion chromatography. In SDS-gel, the sample prior to size exclusion column purification was run on the lane next to the protein standard. The other lanes are corresponding to the different elution volume for the gel filtration profile below. After purification, the fraction 30-36 were collected and used for crystallization experiment.

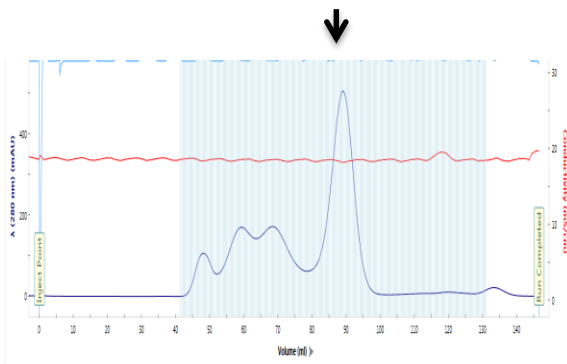
A



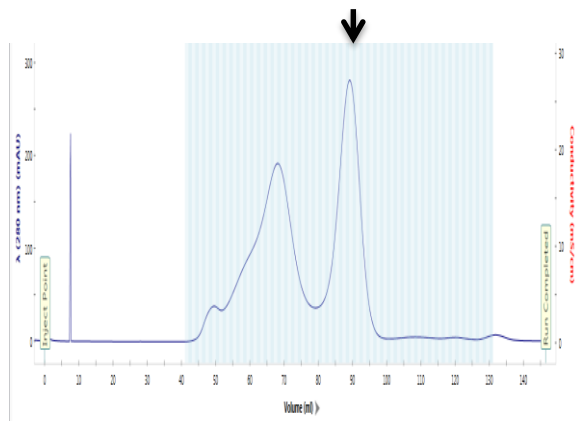
Rtr1₁₋₂₁₃ Y105A gel filtration Profile



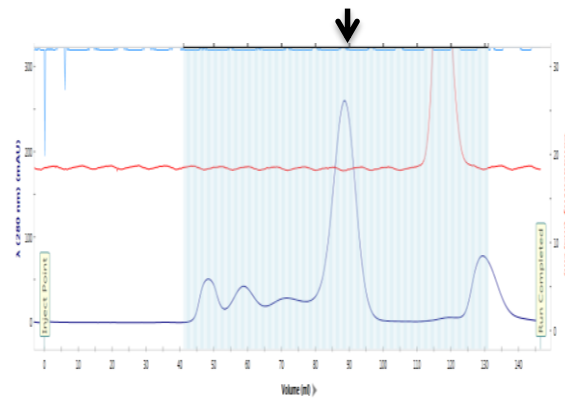
Rtr1₁₋₂₁₃ D62A gel filtration



Rtr1₁₋₂₁₃ D65A gel filtration Profile



Rtr1₁₋₂₁₃ E66A gel filtration



Rtr1₁₋₂₁₃ E66A gel filtration Profile

B

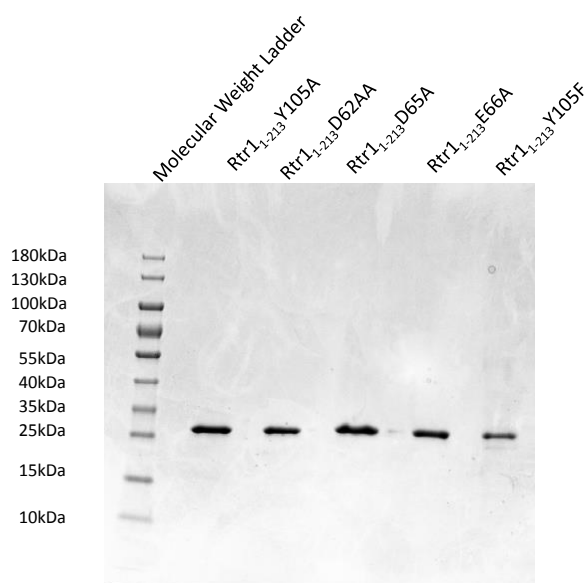


Figure S4: Gel filtration profile and SDS-PAGE electrophoresis of Rtr1₁₋₂₁₃ mutation variants with low in vitro activity. (A) Gel filtration results with arrows indicating the peaks that were collected during elution and used in SDS-PAGE gel in (B).

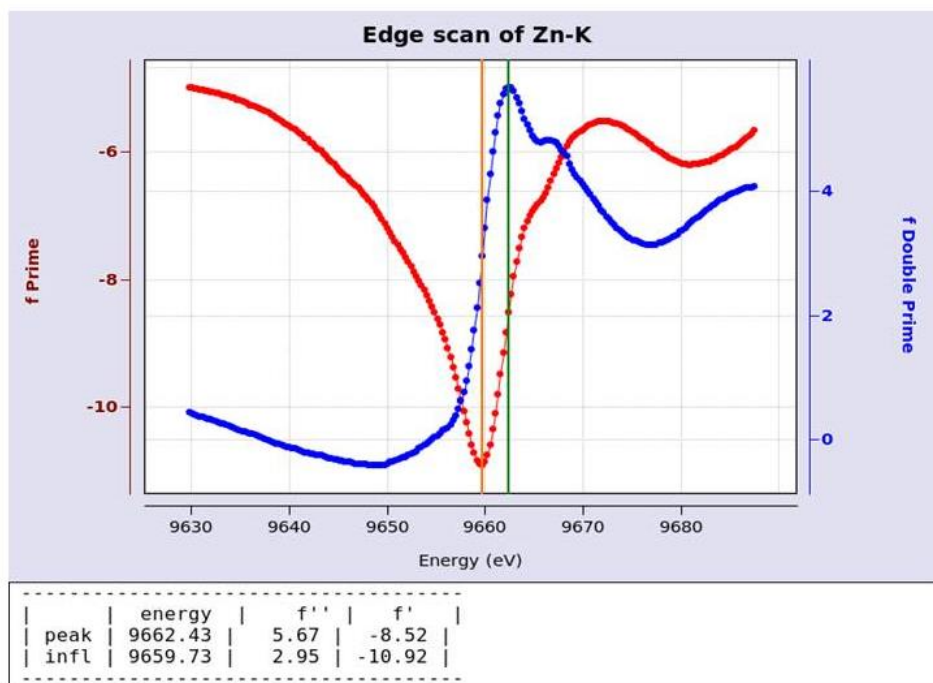


Figure S5: The presence of zinc in Rtr1₁₋₁₇₈ crystals. Analysis of the anomalous absorption edge at 9662.43eV in synchrotron confirmed the identity of the metal ion (zinc) in Rtr1 crystals.

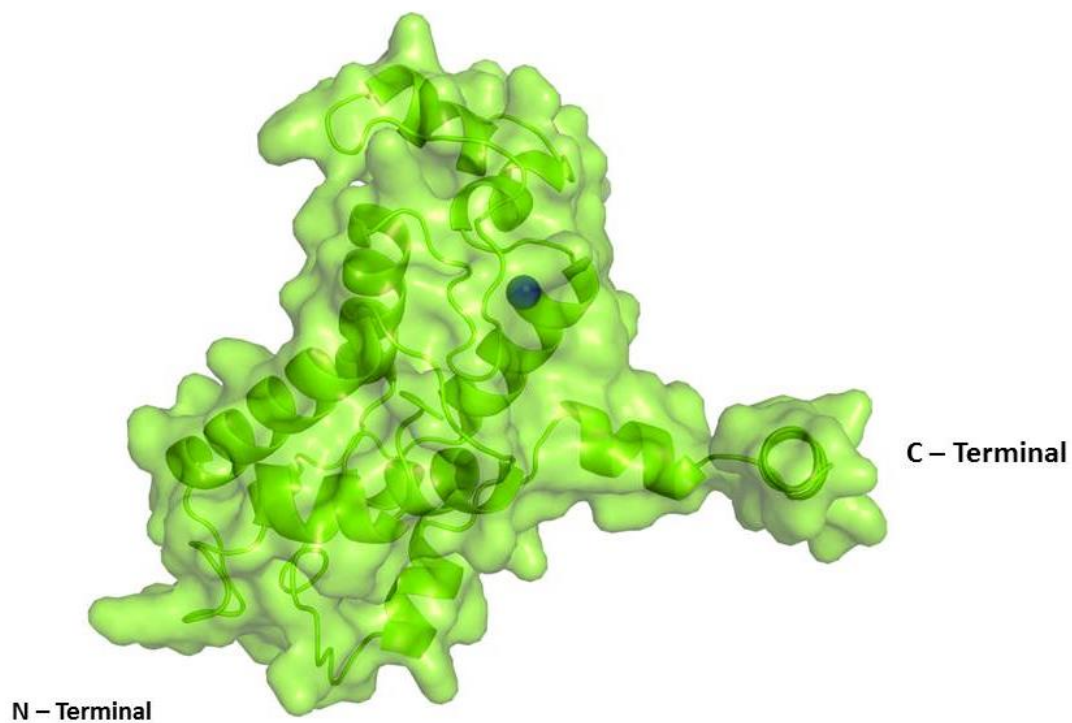


Figure S6: Surface representation of *S. cerevisiae* Rtr1₁₋₁₇₈. One molecule of Rtr1₁₋₁₇₈ from the asymmetric unit. The blue ball represents a zinc ion.

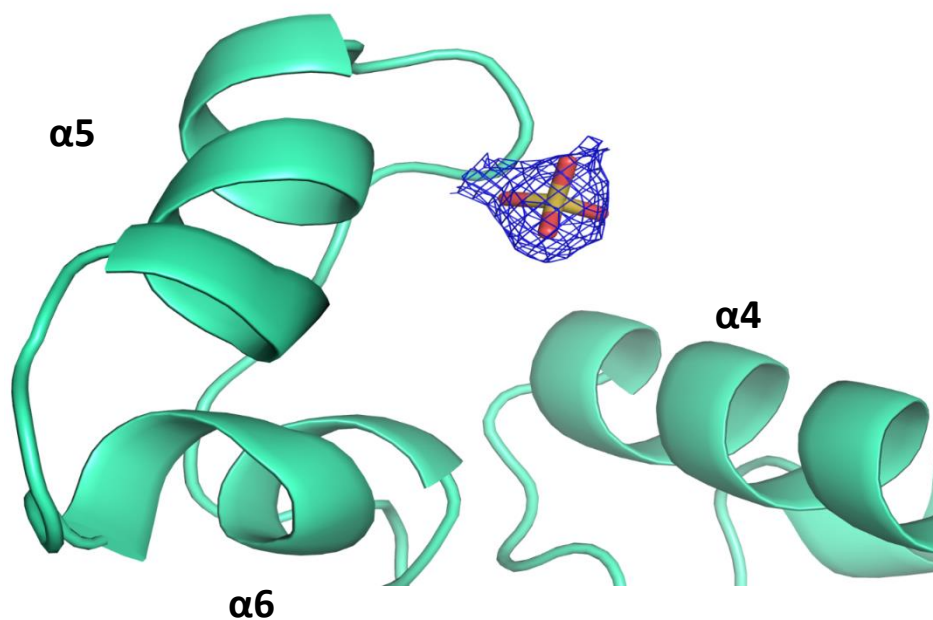


Figure S7: The electron density of sulfate molecule at site 1 in the Rtr1₁₋₁₇₈ structure. The blue mesh represents the 2FoFc electron density contoured to 1 σ . A sulfate ion from crystallization mother liquor is built into the density with good fit.

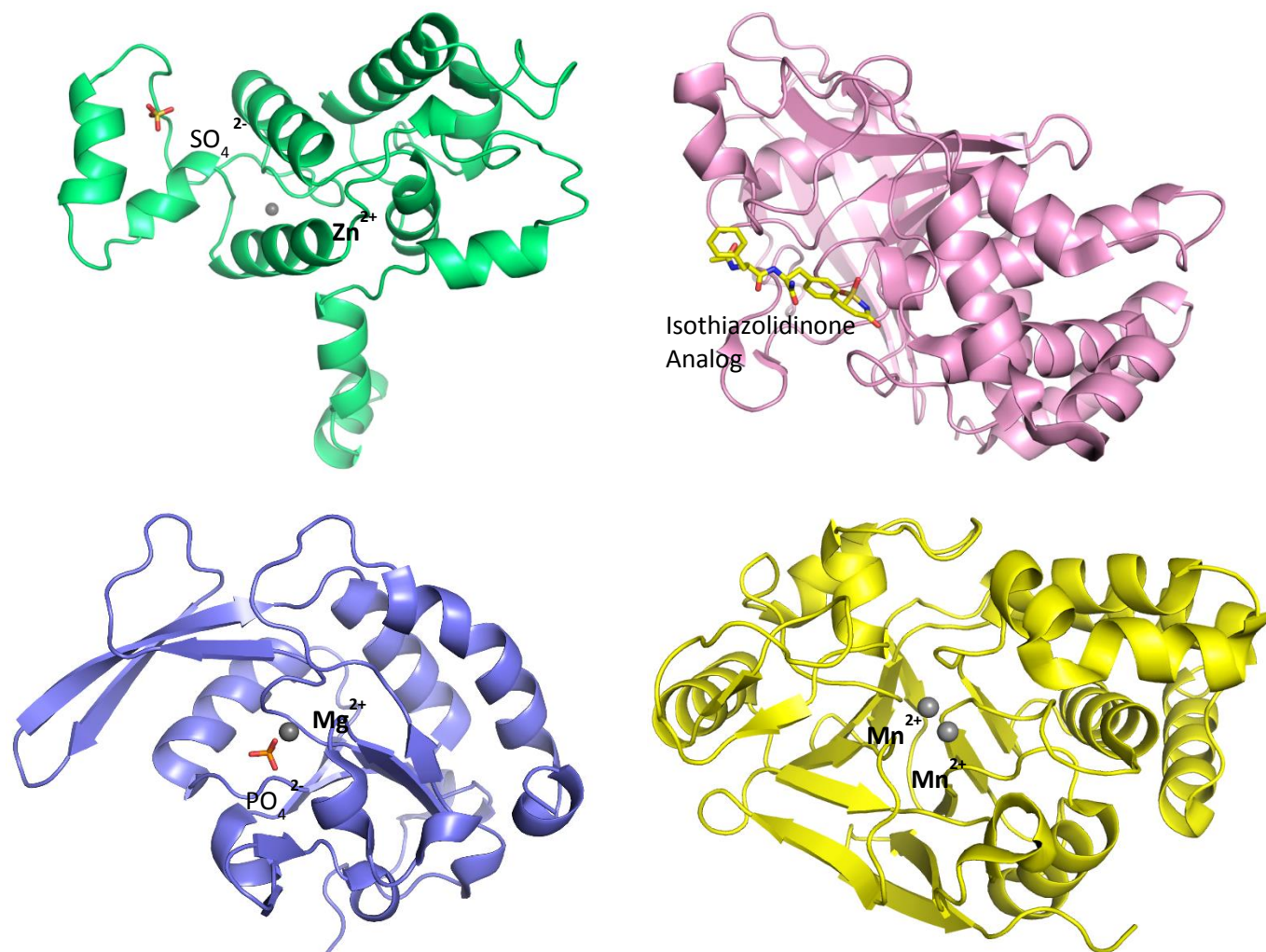


Figure S8: Comparison of protein folding in different phosphatases families. *S. cerevisiae* Rtr1₁₋₁₇₈ is color green with zinc ion shown as a gray sphere and sulfate ion in site 1 shown in stick representation. Cysteine-based phosphatase PTP1b (PDB ID: 2CM7) is pink with stick representation of bound inhibitor. HAD phosphatase Scp1 (PDB ID: 3LOC) is blue with Mg²⁺ ion shown as gray sphere and phosphate shown in stick representation. The catalytic domain of the metal-dependent phosphatase PP2A (PDB ID: 2NYM) is yellow with two Mn²⁺ ions shown as gray spheres.

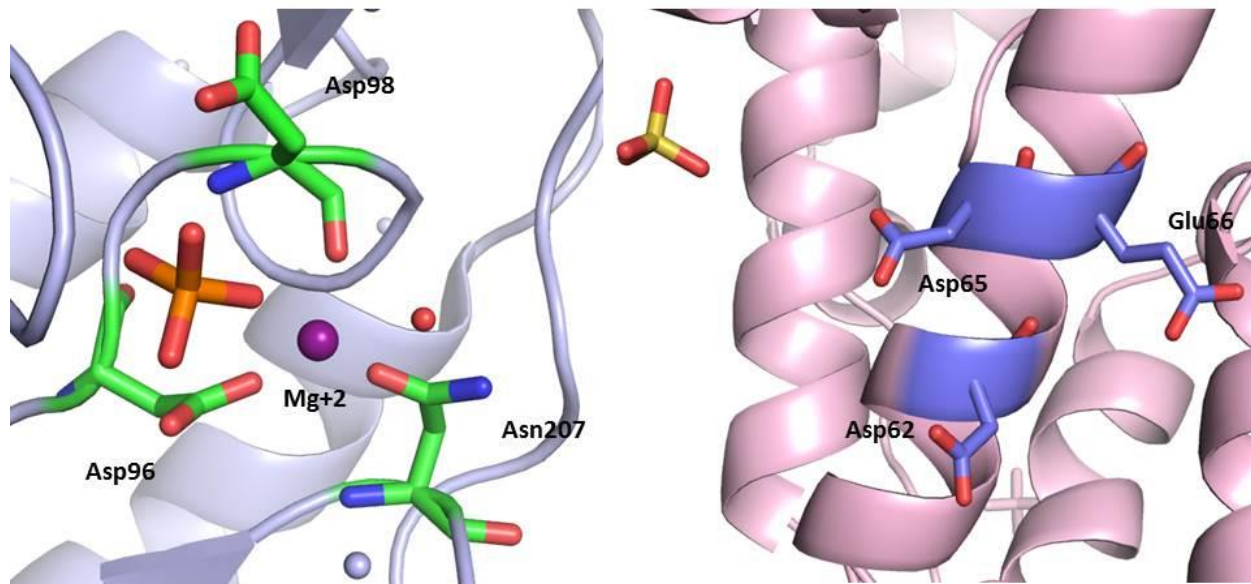


Figure S9: Comparison of the active site of Scp1 and Rtr1. Left shows the DXDX motif in Scp1 (PDB ID: 2GHT), which mediates phosphoryl transfer. Right shows Asp⁶², Asp⁶⁵, and Glu⁶⁶ (DXXDE) in Rtr1, which are important for phosphoryl transfer.

Table S1. Analysis of stability and activity of Rtr1 and the mutants. NA, not applicable. Molecular weight of full-length Rtr1 is 26239 Da, Rtr1₁₋₂₁₃ is 24779 Da, and Rtr1₁₋₁₇₈ is 20853 Da.

Protein	Expressed in <i>E. coli</i>	Detected as a single band of appropriate size by SDS-PAGE	Eluted at appropriate volume in gel filtration chromatography	Activity relative to that of Rtr1 ₁₋₂₁₃
Full-length Rtr1	Yes	Yes	Yes	32.3%
Rtr1 ₁₋₁₂₉	No	NA	NA	NA
Rtr1 ₁₋₁₃₇	No	NA	NA	NA
Rtr1 ₁₋₁₆₇	No	NA	NA	NA
Rtr1 ₁₋₁₇₈	Yes	Yes	Yes	35.8%
Rtr1 ₁₋₂₁₃	Yes	Yes	Yes	100%
Rtr1 ₁₋₂₁₃ C73A	No	NA	NA	NA
Rtr1 ₁₋₂₁₃ C78A	No	NA	NA	NA
Rtr1 ₁₋₂₁₃ C112A	No	NA	NA	NA
Rtr1 ₁₋₂₁₃ H116A	No	NA	NA	NA
Rtr1 ₁₋₂₁₃ D62A	Yes	Yes	Yes	6.3%
Rtr1 ₁₋₂₁₃ D65A	Yes	Yes	Yes	32.8%
Rtr1 ₁₋₂₁₃ E66A	Yes	Yes	Yes	5.5%
Rtr1 ₁₋₂₁₃ Y105A	Yes	Yes	Yes	2.4%
Rtr1 ₁₋₂₁₃ F130A	Yes	Yes	Yes	78%
Rtr1 ₁₋₂₁₃ Y105F	Yes	Yes	Yes	9.5%
Rtr1 ₁₋₂₁₃ R86A	Yes	Yes	Yes	25.2%
Rtr1 ₁₋₂₁₃ K97A	Yes	Yes	Yes	28.4%
Rtr1 ₁₋₂₁₃ H110A	Yes	Yes	Yes	14.3%
Rtr1 ₁₋₂₁₃ R86AK97A	Yes	Yes	Yes	19.2%
Rtr1 ₁₋₂₁₃ R86AK97AH110A	Yes	Yes	Yes	6.0%

Table S2. Analysis of stability and activity of RPAP2. NA, not applicable. Molecular weight of RPAP2₃₂₋₂₇₄ is 27,821 Da; molecular weight of RPAP2₃₂₋₃₄₅ is 35,696 Da.

Protein	Expressed in <i>E. coli</i>	Detected as a single band of appropriate size by SDS-PAGE	Eluted at appropriate volume in gel filtration chromatography	Activity relative to that of RPAP2 ₃₂₋₂₇₄
RPAP2 ₁₋₃₄₅	No	NA	NA	NA
RPAP2 ₃₂₋₂₇₄	Yes	Yes	Yes	100%
RPAP2 ₃₂₋₃₄₅	Yes	Yes	Yes	34.3%
RPAP2 ₃₂₋₂₇₄ Y127A	Yes	Yes	Yes	Not detected